3D analysis of the soil porous architecture under long term contrasting management systems by X-ray Computed Tomography

L.F. Pires[a], W.L. Roque[b], J.A. Rosa[c], S.J. Mooney[d]

[a] *Laboratory of Physics Applied to Soils and Environment, Department of Physics, State University of Ponta Grossa, 84.030-900, Ponta Grossa, PR, Brazil*

[b] *Petroleum Engineering Modelling Laboratory, Department of Scientific Computation, Federal University of Paraíba, 58.051-900, João Pessoa, PB, Brazil*

[c] *Laboratory of Soil Physics, Agricultural Research Institute of Paraná, 84.001-970, Ponta Grossa, PR, Brazil*

[d] Division of Agricultural and Environmental Sciences, School of Biosciences, University of Nottingham, Sutton Bonington Campus, Leicestershire LE12 5RD, UK

Corresponding author:

Prof. Dr. Luiz F. Pires, Phone: (55) 42 3220 3044. Fax: (55) 42-3220-3042

E-mail: lfpires@uepg.br (Luiz F. Pires);

Proofs should be sent to:

Prof. Luiz Fernando Pires, Departamento de Física, Universidade Estadual de Ponta Grossa, Campus de Uvaranas, Bloco L, Sala 15B; Av. Carlos Cavalcanti, 4748, CEP 84.030-900, Ponta Grossa, PR, Brazil.

3D analysis of the soil porous architecture under long term contrasting management systems by X-ray Computed Tomography

L.F. Pires[a,1], W.L. Roque[b], J.A. Rosa[c], S.J. Mooney[d]

[a] *Laboratory of Physics Applied to Soils and Environment, Department of Physics, State University of Ponta Grossa, 84.030-900, Ponta Grossa, PR, Brazil*

[b] *Petroleum Engineering Modelling Laboratory, Department of Scientific Computation, Federal University of Paraíba, 58.051-900, João Pessoa, PB, Brazil*

[c] *Agricultural Research Institute of Paraná, 84.001-970, Ponta Grossa, PR, Brazil*

[d] *Division of Agricultural and Environmental Sciences, School of Biosciences, University of Nottingham, Sutton Bonington Campus, Leicestershire LE12 5RD, UK*

ABSTRACT

The development of adequate soil structure is important for achieving good physical status, which influences the sustainability of agricultural areas. Different management systems lead to the development of a wide range of soil pore network characteristics. The objective of this research was to analyze the effect of three contrasting tillage systems (zero-tillage, ZT; reduced tillage, RT; conventional tillage, CT) in the soil porous system of an Oxisol. Samples were collected from the surface layer (0-10 cm). An area under secondary forest (F) was also assessed to provide an undisturbed reference. X-ray Computed Tomography (μCT) scanning of undisturbed soil samples and image analysis were employed for analysis of the pore network. The soil under ZT

[1] Corresponding author
Tel.: +55 42 3220-3044
E-mail addresses: luizfpires@gmail.com; lfpires@uepg.br (L.F. Pires)

had the smallest porosity in comparison to the other management systems. The conventionally tilled soil had the largest porosity and the most connected pores. One large connected pore was responsible for around 90% of the porosity of the resolvable pores (>35 μm) studied for all the management systems. Pores of elongated shapes, which enhance water movement through the soil, were the most frequent pores in terms of shape.

Keywords: Minimum tillage; Zero-tillage; Conventional tillage; Morphological properties; X-ray microtomography; Soil structure.

1. INTRODUCTION

The use of tillage has been employed for centuries to improve soil structure for enhanced crop development. However, the choice of tillage systems can have a significant impact on a soil heath and quality. Sustainable farming systems greatly depend on soil quality (Bünemann et al., 2018). Soil tillage provokes substantial changes in several soil physical properties such as total porosity, bulk density, water retention and infiltration, penetration resistance, pore size distribution, connectivity and tortuosity (Imhoff et al., 2010; Daraghmeh et al., 2009; Blanco-Canqui et al., 2004; Katsvairo et al., 2002).

In Brazil the adoption of minimum tillage systems such as reduced (RT) and zero tillage (ZT) is common. The total Brazilian area used in crop production is around 66 million hectares and there are over 31 million hectares under ZT (FEBRAPDP, 2013). Conventional tillage (CT) is characterized by the disruption of the top soil due to ploughing and harrowing operations employed to turn over and loosen the soil. As a result of these operations, macropores are created and pore continuity is disrupted, which directly affect the water movement (e.g. hydraulic conductivity and infiltration) and retention (Blanco-Canqui et al., 2017; Ogunwole et al., 2015; Cássaro et al., 2011; Imhoff et al., 2010). Minimum tillage systems such as RT and ZT do not usually lead to

drastic soil structure changes. These systems, known as conservation techniques, have been utilized as a means of reducing tillage and field costs as well as for conserving soil structure due to reduced disturbance (Aziz et al., 2013; Cavalieri et al., 2009). The residues of the previous crop are left intact and the absence of harrowing in ZT and RT can increase soil organic carbon and aggregate stability, reduce CO_2 emissions and moderate fluxes of water, air and heat through the soil (Aziz et al., 2013; Daraghmeh et al., 2009; Zibilske and Bradford, 2007).

The fluxes of water and air, organic matter decomposition, plant-available water and soil resistance to erosion are directly linked to the architecture of the soil porous system. Mesopores and macropores play an important role in these processes (Imhoff et al., 2010; Fuentes et al., 2004; Cameira et al., 2003). In CT, the soil porous system is affected by operations such as ploughing and harrowing, which can increase porosity and loosen soil (Mangalassery et al., 2014). This operation allows good root growth and air exchange, while the exposition of the soil to rain in tropical regions can sometimes lead to erosion (Alvarez et al., 2009). On the other hand, the activity of earthworms and root decay help to create channels and burrows under RT and ZT, which facilitate drainage and gaseous diffusion (Soto-Gómez et al., 2018; Carducci et al., 2017; Pires et al., 2017; Pierret et al., 2002).

Based on the important functions that mesopores and macropores fulfill for a healthy soil, techniques to image and measure key properties such as X-ray Computed Tomography (µCT) are very important (Tseng et al., 2018; Yang et al., 2018; Ferreira et al., 2018; Pagenkemper et al., 2014). The spatial distribution of pores can be non-destructively imaged at high resolutions and in three dimensions (3D) by µCT (e.g. Galdos et al. 2018; Helliwell et al., 2013; Peth et al., 2008). µCT has been previously applied with success to study the size, shape, number, connectivity, degree of anisotropy, macropore thickness, fractal dimension and tortuosity of the soil porous system (Wang et al., 2016; Dal Ferro et al., 2014; Garbout et al., 2013; Vogel, 1997).

This provides vital information to characterize the physical structure of the porous system, which allows a better understanding of key processes (i.e. mass and energy transport, nutrient cycling, root development) within the soil (Hillel, 2004).

Previous studies on evaluating the influence of tillage systems at the µm scale in 3D in tropical soils are still scarce. In Brazil, one of the largest food and agricultural producers of the world, previous studies have characterized the soil porous system at µm to measure the porosity and pore size distribution of Brazilian Oxisols (Vaz et al., 2011), assessed the effect of tillage systems on the percentage of macropores (Beraldo et al., 2014) and explored the spatial and morphological configuration of the pore space of Oxisols under CT (Carducci et al., 2017, 2014). Other studies have determined the influence of ZT on the pore size and shape distribution of macropores (Passoni et al., 2015), tested the capacity of soil recovering under different management strategies (Marchini et al., 2015) and measured the impact of ZT and CT on the pore size and shape distribution and water retention (Pires et al., 2017). Recent work has analyzed the soil structure utilizing the geometrical parameters of the soil porous system (Tseng et al., 2018), considered the influence of liming on the structure of aggregates under ZT (Ferreira et al., 2018) and revealed the structural development associated with long term (>30 years) ZT (Galdos et al., 2018).

The objective of this particular research was to apply the X-ray Computed Tomography technique to evaluate, in 3D and at the µm scale, the morphological properties of an Oxisol under contrasting soil management systems. Experimental areas under long term zero-tillage and reduced and conventional tillage systems were investigated. Samples were collected at the soil surface layer (0-10 cm).

2. MATERIALS AND METHODS

The experimental field plots of this study were located in Ponta Grossa, in a humid mesothermal Cfb-subtropical region in southern Brazil (25°09’S, 50°09’W, 875 m

above sea level) (Cássaro et al., 2011). The soil was an Oxisol (Rhodic Hapludox) with clay texture according to USDA soil taxonomy (Soil Survey Staff, 2013). The experimental areas have long gentle slopes ranging from 2 to 7%. The Oxisol evolved from the clastic sediments of the Devonian period characterized by a mixture of Ponta Grossa shale (MINEROPAR, 2013). Deep and very structured profiles are found in the experimental site characterized by high porosities and good internal drainage (Sá et al., 2015).

Three tillage systems were compared in this study (conventional tillage – CT, reduced tillage – RT and zero-tillage – ZT). An area under secondary forest (F) was utilized as baseline to assess the management-induced changes in soil structure, which is located close to (≈200 m far) the experimental field plots. Some of the key characteristics of the soil (0-10 cm depth) from the experimental areas are shown in Table 1.

The experimental plots studied here have areas of c. 1.0 ha (ZT) and c. 0.6 ha (CT and RT), respectively. The tillage systems had been employed in the areas for over 35 years at the time of sampling. The experimental areas of CT, RT and ZT were initiated in 1981 after conversion of part of secondary forest to pasture-land (Sá et al., 2015). Under CT, the soil was submitted to discing at 25 cm depth followed by 10 cm harrowing twice a year after summer and winter harvest. For the area under RT, the soil was prepared through the use of a chisel cultivator at 25 cm depth followed by a 10 cm narrow disking, causing minimum soil disturbance, and the crop residues were maintained at the soil surface. The area under ZT was not submitted to soil disturbance. In these areas, crop rotation was performed, with cover crops [oats (*Avena strigosa*) or vetch (*Vicia sativa*)] or wheat (*Triticum aestivum L.*) in winter and corn (*Zea mays*) or soybean (*Glycine max*) in summer (Table 2). The operations of soil and crop management, sowing and harvest, were made with commercial tillage machines (e.g. tractor). The traffic in the ZT area was restricted to sowing equipment

129 with a cutting disc for sowing the summer and winter crops. Each experimental area
130 (ZT, CT and RT) was submitted to 8-9 soil interventions through the year (clearing,
131 planting seed and soil preparation operations) using tractors around four tonnes in
132 weight.

133 Soil samples were taken from the 0-10 cm layer after corn harvest in April 2017.
134 For CT, sampling occurred almost six months after ploughing and harrowing
135 operations, which allowed the sampling of natural reconsolidated structures. ZT, RT
136 and F samples were also taken at the same sampling time. Core samples of 91 cm^3
137 (5.0 cm high and 4.8 cm inner diameter) were collected in steel cylinders with an
138 Uhland core sampler (Folegatti et al., 2001). Three samples of each tillage system and
139 forest (3 samples × 4 systems) were collected for the macroporosity and microporosity
140 analyses and other five samples (5 samples × 4 systems) for the µCT analysis (Table
141 1). After sampling, the samples were wrapped in plastic foil and transported to the
142 laboratory. The soil excess outside the steel cylinders was carefully trimmed off and top
143 and bottom surfaces of the sample were made flat to ensure that the soil volume was
144 equal to the internal volume of the cylinder. This procedure was carried out with the
145 help of a palette knife.

146 Samples were collected very carefully, in order not to introduce soil compaction
147 during extraction and handling of the steel cylinders. To minimize damages in the soil
148 structure due to the force required for collection, samples were taken some days after a
149 high intensity rainfall event with the soil near its plastic limit. For organic carbon (3
150 samples × 4 systems) and texture (3 samples × 4 systems) measurements, disturbed
151 soil samples were collected at three different points. Soil organic carbon was
152 determined by the Walkley-Black method and texture by the hydrometer method (Gee
153 and Or, 2002; Nelson and Sommers, 1982).

154 The soil samples were carefully extracted from the steel cylinders before the
155 µCT scans. Prior to the scanning, the samples were coated with paraffin wax for

transport to the United Kingdom. Each soil sample was scanned using a GE v|tome|x m X-ray µCT scanner (GE Measurement & Control Solutions, Wunstorf, Germany) at the Hounsfield Facility (The University of Nottingham, Sutton Bonington Campus, U.K.). The voltage, current and integration time adopted for the image acquisition process were 180 kV, 160 µA and 250 ms. A 0.1 mm Cu-filter was used to minimize beam-hardening effects. A total of 2520 projections were obtained per sample with a pixel resolution of 35 µm. Therefore, it was not possible to quantify pores below the resolution mentioned.

The radiographs of each scan were reconstructed in 32 bit format in order to avoid compression of the greyscale histogram. After reconstruction the images were imported into Volumetric Graphics (VG) StudioMAX® 2.0 and cropped (i.e. resized) to a cubic shape with 30.1 × 30.1 × 30.1 mm^3 (860 × 860 × 860 pixels). The image cropping was carried c. 10 mm away from the borders of the samples to avoid possible artifacts on the edge of the soil core samples that may have arisen from sampling or transport.

The original grey-level µCT images were processed using ImageJ 1.42 software (Rasband, 2007). A *3D median* filter with radius of 2 voxels was applied to reduce noise in the images. Subsequently, an *unsharp mask* with standard deviation of 1 voxel and weight of 0.8 was applied to emphasize edges. The segmentation process was based on the nonparametric and unsupervised Otsu method of thresholding (Otsu, 1979). The *remove outlier* tool with radius of 0.75 was applied in the images after segmentation. The images were also visually inspected to verify the quality of the segmentation procedure. This resulted in a binary image, in which pores and solids were respectively represented by white and black pixels.

For the 3D structure analysis, soil pores were classified according to their shape and size distribution. For the shape classification, parameters known as major, intermediate and minor axes of the ellipsoids that represent each pore were

183 determined by using 3D measuring techniques (Borges et al., 2018; Pires et al., 2017).
184 These parameters were measured by using the *Particle Analyser* tool in the ImageJ.
185 The soil pores were classified according to Zingg (1935) based on the relations of the
186 intermediate by the major (Int./Maj.) and of the minor by the intermediate (Min./Int.)
187 axes. Equant (EQ), Prolate (PR), Oblate (OB) and Triaxial (TR) shaped pores were
188 analyzed (Ferreira et al., 2018; Pires et al., 2017) (Table 3). When one of the axes of a
189 specific pore could not be determined, this pore was not classified (unclassified pore)
190 according to its shape. These pores are generally associated with enhanced
191 complexity of individual pores, which means that a geometrical shape cannot be fitted
192 for them.

193 3D porosity was determined for all pores >8 voxels and the total number of pore
194 voxels within the region of interest. Isolated pores smaller than 9 voxels were removed
195 from the porous fraction of the images in the quantitative analyses to avoid
196 misclassification from unresolved voxels (Jefferies et al., 2014). The total number of
197 isolated pores within the region of interest was utilized for the 3D pore size distribution
198 based on the volume of pores (0.0004-0.01, 0.01-0.1, 0.1-10 and >10 mm^3) (Ferreira et
199 al., 2018; Pires et al., 2017).

200 The network tortuosity and connectivity of the pores were calculated using
201 Osteoimage software (Roque et al., 2009). Tortuosity was determined through the
202 geodesic reconstruction algorithm implemented by Roque et al. (2012). The pore
203 network degree of connectivity was estimated by the Euler-Poincare Characteristic
204 (EPC). EPC is a topological property of geometric objects and one of the Minkowski
205 functions used for describing the connectivity of spatial structures (Katuwal et al.,
206 2015). This parameter for a 3D structure is related to the number of isolated parts
207 minus the connectivity of an object (Thurston, 1997). To estimate the EPC, a stack of
208 serial sections called dissectors (Sterio, 1984) is used. In our study 859 disectors were
209 analyzed for each sample. EPC by the volume of dissectors (EPC_V) was then

calculated for each sample after the images had been previously submitted to the Purify procedure in Bone J plugin (Toriwaki and Yonekura, 2002; Odgaard and Gundersen, 1993). For EPC_V a positive value indicates a poorly connected structure while a negative value suggests a more connected structure (Vogel and Kretzschmar, 1996). The Euler number was also utilized to evaluate the connectivity of the main pore network (i.e. the largest pore). The degree of anisotropy, which gives the preferred orientation of pores, was determined in 3D by using the BoneJ plugin (Doube et al., 2010).

Differences in the soil morphological parameters due to the treatments were evaluated by a one-way analysis of variance (ANOVA) followed by Tukey's HSD post hoc tests. Results were classified as statistically significant at $p<0.05$. Parameters such as the mean, standard deviation and coefficient of variations were also measured for each soil physical property analyzed. Pearson correlations among each pair of variables were measured for some of the morphological properties. The statistical analysis was carried out using PAST software (Hammer et al., 2001).

3. RESULTS AND DISCUSSION

Representative 3D images of the soil porous system from the different management systems are presented in Fig. 1. The undisturbed samples collected at the surface layer for the contrasting tillage systems possessed a main pore network composed of connected pores. The 3D images show that the soil under CT seemed to have a high proportion of small connected pores in relation to F, ZT and RT (Fig. 1). The numerous pores observed for the soil under CT suggest this management system was characterized by higher soil porosity than the other treatments. Larger soil pores were observed for the soil under F, ZT and RT, which may be an indication of biological activity. The existence of biopores in areas under forest or conservation management systems is usually associated with the action of earthworms and root penetration (Peth et al., 2008). Normally these biopores tend to be vertically oriented, continuous and

round shaped (Pagenkemper et al., 2015). Earthworm activity in the soil modifies its structure and can affect the transport and exchange processes such as preferential flows and lateral water movement (Rogasik et al., 2014).

Porosities calculated from binary images were higher for CT compared with the other management systems (Fig. 2a). Porosity was c. 2.3 times higher for CT than ZT. Significant differences ($p<0.05$) were observed for ZT in relation to the other management systems. The number of pores was significantly different between CT, F and ZT (Fig. 2b). The soil under ZT had the highest number of pores followed by F, RT and CT. The number of disconnected pores was c. 1.5 times higher for ZT than CT.

The lowest porosity observed for ZT maybe associated with a “zero-tillage pan”, which can happen in areas under long term ZT as previously observed in the South of Brazil down to 20 cm soil depth (Mazurana et al., 2017; da Silva et al., 2009; Klein and Libardi, 2002). According to Reichert et al. (2007), soil compaction in ZT can occur mainly when this practice is utilized for long periods due to machinery traffic, low soil mobilization and natural soil arrangement. One of the consequences of this densification is the reduction of macroporosity and the increase in microporosity (da Silva et al., 2016; Mangalassery et al., 2014). Similar findings for areas under ZT close to the experimental plots studied were observed by Borges et al. (2018) and Pires et al. (2017) for samples collected in different periods of time. Normally, for soils under ZT it is expected that the traffic effects can be compensated by the creation of macropores originating from the fauna activity, high organic content and root development, but this was not observed in this study. Similar results were recorded by Blanco-Canqui et al. (2017) and Soracco et al. (2012).

The large porosity observed under CT is probably associated with the soil loosening and disturbance, which favours the formation of macropores at the surface layer (Jabro et al., 2009). Conventional management can cause an increase in the volume of pores, permeability and air flow, which is related to the harrowing and

ploughing operations (Rossetti et al., 2013). For the soil under RT, the porosity can be explained by reduced soil disturbance combined with the incorporation of residues from previous crops for this management (Cunha et al., 2015). In terms of porosity, this management presents the most similar results to the reference area (F).

The smallest number of pores was for the soil under CT, which was unexpected (Fig. 2b). The aggregate breakdown induced by harrowing and ploughing operations normally increases the number of pores due to the loosening effect of conventional management systems. Several previous studies have demonstrated that systems with ploughing are characterized by looser soil structures (Dal Ferro et al., 2014; Garbout et al., 2013; Munkholm et al., 2012; Munkholm and Hansen, 2012). Borges et al. (2018) and Pires et al. (2017) also observed a larger number of pores for the soil under CT than ZT for the same experimental area. A possible explanation for the smaller number of pores observed under CT in the current study could be the soil resettling, which is induced by the local wetting and drying cycles, caused by rainfall and dry periods and biological activity including root growth (Daraghmeh et al., 2009).

The contrasting management systems did not demonstrate significant differences in the degree of anisotropy though it was highest in RT, followed by ZT and CT, whereas F had the smallest value (Fig. 2c). This parameter was c. 1.7 times higher for RT than F. The results of degree of anisotropy obtained in this study are in line with those presented by Dal Ferro et al. (2014). These authors obtained values of 0.21 (CT) and 0.25 (ZT) for samples from the topsoil (0-10 cm). However, there was no pattern between the results of degree of anisotropy and porosity among the different management approaches. Strong linear positive and negative correlations were observed for RT ($r=0.63$), and ZT ($r=-0.60$) and F ($r=-0.86$) between these two parameters, which shows that the soil under ZT presented similarities with F. The smallest degree of anisotropy obtained for F indicates a more isotropic porous system, which means that pores are not oriented in particular directions and there are

291 similarities in the pore orientation in the different directions analyzed (Hernández
292 Zubeldia et al., 2016). Therefore, this kind of porous system does not present a
293 tendency for preferential flows but is expected that the water can infiltrate and also
294 redistribute into the soil in all directions in similar conditions as per Darcy's Law. Tseng
295 et al. (2018) also observed small values for the degree of anisotropy for a native forest
296 area in comparison to degraded or recovering pasture land. The degree of anisotropy
297 data indicated that all management systems had a good physical condition as far as
298 water infiltration is concerned. For comparison, Tseng et al. (2018) observed values of
299 0.64 for an area of degraded soil and Garbout et al. (2013) of 0.37 for a direct drilling
300 management system.

301 The pore connectivity measured by the volumetric Euler-Poincaré Characteristic
302 was lowest for CT followed by RT, F and ZT (Fig. 2d). Significant differences ($p<0.05$)
303 of this parameter were observed only between CT and ZT. For these two management
304 systems the increase in pore connectivity was also followed by the increase in the
305 degree of anisotropy (strong linear positive correlations: $r=0.74$ for CT and $r=0.60$ for
306 ZT) of the soil porous system, which indicates slight differences in the spatial
307 characteristics of the pores in some specific direction in the images (Tseng et al.,
308 2018). The same tendency of the volumetric Euler-Poincaré Characteristic was found
309 for the pore connectivity (Euler number) of the largest pore (CT<RT<F<ZT), which was
310 c. 2.8 times smaller for CT than ZT (Fig. 2e). Surprisingly, the highest pore connectivity
311 was observed for the soil under CT. We expected that the breakdown of aggregates
312 should decrease the pore connectivity due to soil loosening as observed by Dal Ferro
313 et al. (2014). However, as the samples were collected months after ploughing and
314 harrowing operations, the reorganization of the soil particles and aggregates, as
315 function of the corn root system and weather conditions, may favour the connectivity of
316 the pores under CT (Strudley et al., 2008). Muñoz-Ortega et al. (2015) observed that

317 soils under tilled areas can present structures similar to natural conditions, which can
318 lead to highly connected porous systems.

319 From a visual inspection of the 3D images (Fig. 1), we observed that all the
320 management systems presented a main, highly connected pore network. The results of
321 the volumetric Euler-Poincaré Characteristic and Euler number indicate that the soils
322 with the largest porosity had the best pore connectivity, which can be associated with
323 the junction of few large pores with many tunnels or a high amount of small connected
324 pores (Vogel, 1997). Although, there was no clear relation between overall porosity and
325 soil pore connectivity (results not shown), which indicates that probably other physical
326 properties have a greater influence on the pore connectivity than the porosity. In the
327 case of ZT and RT, it was expected that the pore connectivity was mainly associated
328 with the biological activity, root decay and low or nonexistent soil disturbance (Aziz et
329 al., 2013; Daraghmeh et al., 2009; Zibilske and Bradford, 2007). Continuous pores can
330 be produced by crack formation, earthworm activity or retention of crop residues
331 maintained after harvesting on the soil surface, which act as physical barriers making
332 the soil less susceptible to erosion or the pressure of agricultural machine traffic under
333 crop residue harvest (Imhoff et al., 2010). In the case of RT, the soil cutting induced by
334 chiseling preserves cracks and channels between aggregates, which creates inter-
335 connected pores with large volumes (Peña-Sancho et al., 2017). Despite low porosity
336 observed for ZT, pore connectivity was positively influenced by the organic matter
337 content at the soil surface, which may have compensated the negative influence of
338 macroporosity reduction (Franzluebbers et al., 2011). Martins et al. (2011), working at
339 the same experimental area of our study, found differences of around 42% in the
340 carbon content at the topsoil between CT and ZT after 27 years of management.

341 The results obtained here for porosity and pore connectivity are extremely
342 valuable due to the importance of the mesopores and macropores for water infiltration
343 and retention. Changes in the soil porous system induced by tillage can present

344 significant modifications in the hydraulic properties of the soil as pointed out by Alvarez
345 et al. (2009), Daraghmeh et al. (2008) and Buczko et al. (2006). The importance of soil
346 structure to conserve the quality and the health of the soil, reduce net CO_2 emissions,
347 and increase organic carbon pools is another vital aspect for the micrometric
348 characterization of this porous system; conventional and conservational management
349 systems play an important role in all of these processes (Zibilske and Bradford, 2007).

350 The soil pore system tortuosity was calculated for different directions (x,y,z),
351 and an average tortuosity was obtained considering the three directions together (Fig.
352 3). The calculation of tortuosity for different directions is related to the influence of this
353 parameter for the movement of water and air through the soil. This movement occurs in
354 all directions across the soil, and changes in the soil porous system in one direction
355 certainly have the possibility of inducing preferential flows in the soil profile. Significant
356 differences ($p<0.05$) in the average τ was observed between CT and F, and ZT (Fig.
357 3a). The lowest average tortuosity was measured for ZT, followed by RT, CT and F.
358 Porosity and average tortuosity were strongly correlated only for F ($r=0.78$) and ZT
359 ($r=0.77$), which indicates an increase in pore complexity with an increase in porosity for
360 these two cases. The presence of crop residues in decomposition in ZT and soil fauna
361 in F can help to explain these results (Franzluebbers et al., 2011).

362 The tortuosity in the x- and y-directions was the highest in F, followed by CT
363 and RT, then ZT (Figs. 3b,c). Significant differences were found only between F and ZT
364 for both tortuosity directions. Porosity and x- and y-direction tortuosities were strongly
365 correlated for all the management systems ($r=0.86$ for CT; $r=0.93$ for RT; $r=0.88$ for ZT
366 – x-direction tortuosity and $r=0.87$ for CT; $r=0.78$ for RT; $r=0.93$ for ZT – y-direction
367 tortuosity) and F ($r=0.90$ – x-direction tortuosity and $r=0.83$ – y-direction tortuosity). In
368 general, the results of x- and y-direction and average tortuosities had the same
369 tendency among management systems. The tortuosity in the z-direction was not
370 characterized by significant differences between F, CT and RT, whereas ZT was

371 different from F (Fig. 3d). The highest z-direction tortuosity was observed for F,
372 followed by RT, CT and ZT. The average tortuosity as well as that in the x-, y- and z-
373 directions was c. 1.1 times higher for F than ZT. Porosity was strongly correlated to z-
374 direction tortuosity only for F (r=0.86) and weakly correlated for CT (r=0.17), which was
375 probably associated with the soil loosening and disturbance in the last case (Munkholm
376 et al., 2012; Munkholm and Hansen, 2012).

377 The lowest average tortuosity was in the ZT soil indicating that pores are more
378 aligned for this management. The same results were found for the tortuosity in the
379 different directions. Usually, more aligned pores can sometimes be associated with a
380 better interconnected network of more continuous flow channels (Peth et al., 2008).
381 However, the better alignment of the pores for ZT did not result in a better pore
382 connectivity as observed by the weak linear negative correlation between average
383 tortuosity and volumetric Euler-Poincaré Characteristic (r=-0.22). This means that the
384 more aligned and continuous pores possibly were not interconnected with other pore
385 networks. Tortuosity is mainly related to the degree of complexity of the sinuous porous
386 path (Pagenkemper et al., 2014; Rezanezhad et al., 2010). Despite the better
387 connectivity measured for CT compared to the other management systems, this
388 connectivity is probably associated with the junction of small pores as observed in the
389 3D images (Muñoz-Ortega et al., 2015; Vogel, 1997). Therefore, the highest tortuosity
390 observed for CT in comparison to ZT is possibly related to a higher number of
391 connected small pores. Similar findings were found by Borges et al. (2018) and Peth et
392 al. (2008). The highest tortuosity was measured for the soil under F, which can be
393 associated with the complexity of the soil porous system due to biological activity, soil
394 fauna (insects), roots, a greater amount of residues (tree leaves) maintained at the soil
395 surface and the absence of tillage (Blanco-Canqui and Lal, 2007).

396 The tortuosity of pores in the z-direction directly corresponds to the variation in
397 soil structure associated with soil depth. The more aligned pores in this direction can

be associated with wider and more continuous flow channels, which can improve the water infiltration in this direction. The effective transport of fluids through the pore networks is not only dependent on their continuity but also on their tortuosity (Peth et al., 2008). The similarities in the values of tortuosity for the different directions indicate that the pore complexity follows a similar pattern in all directions analyzed. However, average tortuosity was strongly negatively correlated to the degree of anisotropy for CT (r=-0.90), ZT (r=-0.72) and F (r=-0.66), which means that the presence of more tortuous pores does not necessarily affect the distribution of pores.

In general, the tortuosity data described well aligned pores for all the management systems studied. This result is important because the tortuosity is associated with the hydraulic conductivity. This parameter indicates increased resistance to flow, which means high tortuosity can negatively affect the capacity of soil to water transport (Rezanezhad et al., 2010).

The pore morphology characterized by the shape of pores is similar to the other parameters studied in that it directly affects the movement of water, air and the development of roots through the soil. Changes in the shape of pores due to management will influence the water retention and the amount of water available to plants. The highest contribution of equant (e.g. equant spheroid) shaped pores to the total porosity was observed for F, followed by RT, CT and ZT (Fig. 4a). The proportion of equant shaped pores was c. 1.3 times higher for F than ZT. Significant differences ($p<0.05$) were identified between F, ZT and CT. For prolate (e.g. prolate spheroid / rod) shaped pores (Fig. 4b), the highest contribution to porosity was found for RT, followed by F, ZT and CT. The proportion of prolate shaped pores was c. 1.1 times higher for RT than CT. No significant differences were recorded between management systems for this type of pore shape. The highest contribution of oblate (e.g. oblate spheroid / discoid) shaped pores to porosity was measured for F, followed by CT, RT and ZT (Fig. 4c). The proportion of oblate shaped pores was c. 1.3 times higher for CT than ZT.

Similar to the results of prolate shaped pores, no significant differences were observed between the different management systems. The highest contribution to porosity was verified for pores of triaxial (e.g. blade) shape (Fig. 4d). The following sequence among management systems was found for triaxial shaped pores: F<RT<CT<ZT; and the proportion of them was c.1.1 times higher for ZT than F. Significant differences were observed between F, ZT and CT.

The presence of slightly to very flat/elongated (e.g. prolate, oblate and triaxial) pores was greatly influenced by different soil management systems. The presence of earthworms and insects, mainly at the soil surface, will contribute to the appearance of elongated pores (Jarvis et al., 2017; Pagenkemper et al., 2015; Rogasik et al., 2014). According to Pagliai et al. (2004), elongated continuous pores affect plant growth by easing root penetration and increasing the transmission and storage of water and gases. The smallest proportion of platy and equant shaped pores is an indication of a good soil structure (Pagliai et al., 2004; Bouma et al., 1977). The largest proportion of slightly to moderately flat/elongated pores is indicative of soil quality, since they are generally related to the biological activity of living organisms and roots (biopores) (Carducci et al., 2014; Lima et al., 2005). The Euler number showed moderate (r=0.52 for ZT) to strong (r=0.76 for CT and r=0.84 for RT) positive correlations in relation to the contribution of triaxial shaped pores to porosity, which means that the largest presence of these type of pores can positively contribute to water infiltration. However, samples of F had only weak correlation (r=0.17) between these two morphological properties, which can be associated with the increased complexity of the porous system. We observed that the average tortuosity was strongly correlated (r=0.67) to the triaxial shaped pores contribution to the porosity for F. In conventional management, the presence of elongated pores is usually associated with planar shaped pores surrounding or separating aggregates or clods (Pagliai, 1994). The recovery of soil structure, which occurs in soils managed under conventional management systems

after months of ploughing and harrowing operation procedures, can also be identified by an increase in the proportion of elongated pores (Zhao et al., 2017). The largest amount of equant shaped pores in F can also be related to the biologic activity. This pore type also plays an important role in the transport and retention of water, since water can infiltrate very quickly in tubular pores (Yang et al., 2018). A strong positive correlation (r=0.61) was found between the volumetric Euler-Poincaré Characteristic and the contribution of equant shaped pores to porosity for F, which highlights the importance of this type of pore in native or secondary forests.

A large portion of the pores were not classified in terms of shape. The contribution of unclassified pores to porosity was around 60% for F and RT, 66% for ZT and 63% for CT, respectively. Moderate to strong positive correlations were found between the volumetric Euler-Poincaré Characteristic and the contribution of unclassified pores for all the management systems (r=0.58 for ZT, r=0.91 for CT and r=0.85 for RT) and F (r=0.56). As unclassified pores were responsible for a considerable part of the porosity, their contribution to pore connectivity is important and suggests the samples analyzed are characterized by good structural quality. Unclassified pores are also an indicative of the complexity of the soil porous system. The well connected pore structures observed in the 3D images give an idea of the complexity of the soil porous system (Fig. 1). Similar results of a high contribution of complex pores to the overall porosity have also been previously measured for Brazilian soils (Ferreira et al., 2018; Borges et al., 2018; Costa et al., 2018; Pires et al., 2017; Passoni et al., 2015).

The small pores (from 0.0004 to 10 mm^3) made only a small contribution to overall porosity. The highest contribution to porosity for 0.0004 to 0.01 mm^3 pores was observed in ZT, followed by F, RT and CT. Significant differences ($p<0.05$) were recorded between management systems for this pore size interval (Fig. 5a). Porosity displayed strong negative correlations to the interval of pore volumes between 0.0004

and 0.01 mm^3 for F (r=-0.79), CT (r=-0.94) and RT (r=-0.99). For the pore sizes of 0.01 to 0.1 mm^3 (Fig. 5b), significant differences were observed between ZT and the other management systems. Porosity also displayed strongly negative correlations to the interval of pore volumes between 0.01 and 0.1 mm^3 for F (r=-0.90), CT (r=-0.92) and RT (r=-0.89). For the last two size intervals of pores, the increase in porosity was followed by a decrease in the contribution of small pores, which highlights the great contribution of large pores to the overall soil porous system of F, CT and RT studied. The correlation between porosity and the two previous pore size intervals analyzed was moderate to weak for ZT (r=-0.41 for 0.0004 to 0.01 mm^3 and r=-0.29 for 0.01 to 0.1 mm^3). This result shows that the variation in porosity was not greatly influenced by changes in the distribution of small pore sizes for this management.

The highest contribution to porosity for 0.1 to 10 mm^3 pores was observed for ZT, followed by F, RT and CT (Fig. 5c). Similar to the results observed for the 0.01 to 0.1 mm^3, significant differences were found only between ZT and the other management systems. For the largest pores (>10 mm^3), the greatest contribution to porosity occurred for CT, followed by RT, F and ZT. The soil under ZT presented significant differences in comparison to the other management systems (Fig. 5d). The proportion of different pore volume intervals to porosity was c. 3.5 (0.0004 to 0.01 mm^3), c. 4.3 (0.01 to 0.1 mm^3) and c. 4.0 (0.1 to 10 mm^3) times higher for ZT than CT and c. 1.1 times higher for CT than ZT for the largest pore sizes (>10 mm^3) studied.

We observed that in general the samples with high porosities were also characterized by a large contribution of the biggest pores (>10 mm^3) to the porosity, which was corroborated by the strong positive correlations obtained for F (r=0.82), CT (r=0.93) and RT (r=0.94) between these two soil physical properties. This is an indication of highly connected pore networks supported by the moderate to strong negative correlations between the volumetric Euler-Poincaré Characteristic and the

505 contribution of pores >10 mm^3 to porosity for ZT (r=-0.73), CT (r=-0.81) and RT (r=-
506 0.50) of the soil samples analyzed.

507 In terms of pore size distribution, the contribution of pores <10 mm^3 to porosity
508 was around 4% for F, 8% for ZT, 2% for CT and 3% for RT. This indicates that a large
509 part of the porosity is composed of large inter-aggregate pores as observed by Costa
510 et al. (2018). Ferreira et al. (2018) recently showed that >90% of porosity for a soil
511 under ZT consisted of a main pore network as observed in our study. This type of pore
512 system is related to soil structural development and it is indicative of structures that
513 function well for water infiltration (Bullock and Thomasson, 1979). Borges et al. (2018)
514 and Pires at al. (2017) obtained similar results for the same experimental area.
515 Cássaro et al. (2011), in another work in the same site, identified a great concentration
516 of large pores under ZT and CT management systems. The greatest contribution of
517 unclassified pores to porosity is also indication of the presence of a main pore network
518 composed by large pores (Costa et al., 2018; Jefferies et al., 2014). Garbout et al.
519 (2013) determined that the volume of connected pores constituted 91% and 85% for
520 drilling and ploughing areas, which indicates the great contribution of a main pore
521 network to the overall porosity. Dal Ferro et al. (2014) also observed a contribution of
522 around 70% of macropores to porosity, which would contribute to water infiltration and
523 potentially reduce erosion (Imhoff et al., 2010).

524 # CONCLUSIONS

525 We analyzed the structure of samples of an Oxisol under different management
526 systems using X-ray Computed Tomography. The qualitative results obtained through
527 3D visual image analysis showed that the soils under all the management systems
528 (zero-tillage, conventional tillage and reduced tillage) and forest are generally
529 composed of a large main pore network which is highly connected. The pore
530 connectivity results demonstrated that even for ZT, which was characterized by a lower
531 comparable mesoporosity and macroporosity, the soil porous system has a strongly

connected pore network compared to the forest. We attribute this lower porosity for ZT to a possible development of a zero-tillage pan. However, the results of pore connectivity, degree of anisotropy and tortuosity show that the soil structure under ZT was not negatively affected by the reduction in its porosity. The smallest average tortuosity and the largest contribution of triaxial shaped pores found for ZT can help to explain the pore connectivity results. A moderate positive correlation was also measured between the volumetric Euler-Poincaré Characteristic and the unclassified pores for ZT similar to the results of F. As a great part of the porosity was comprised of unclassified pores for all the management systems and forest, these pores present an important contribution to the overall pore connectivity. The largest proportion of elongated shaped pores also demonstrated that all the management systems examined had positive effects in the quality of the soil porous system. Similar to the 3D image visualizations, the largest contribution to porosity was due to the presence of a main pore network, which means the porous system was well connected in all the management systems. The results of this study provided a detailed characterization of the soil porous system at the micrometric scale. This type of information is extremely important due to the relevance of mesopores and macropores in the transport of mass and energy through the soil. We can conclude that each of the management systems studied here presented positive indications of soil quality, which is surprising given their differences in operation and extremely important from an environmental and agricultural points of view.

ACKNOWLEDGEMENTS

LFP would like to acknowledge the financial support provided by the Brazilian National Council for Scientific and Technological Development (CNPq) and the Coordination for the Improvement of Higher Education Personnel (Capes) through the Grants 303726/2015-6 (Productivity in Research) and 88881.119578/2016-01 (Visiting

Scholar). We acknowledge the helpful laboratory and computational work from Dr. Brian Atkinson.

REFERENCES

Alvarez, C.R., Taboada, M.A., Gutierrez Boem, F.H., Bono, A., Fernandez, P.L., Prystupa, P., 2009. Topsoil properties as affected by tillage systems in the rolling Pampa region of Argentina. Soil Sci. Soc. Am. J. 73, 1242–1250.

Aziz, I., Mahmood, T., Islam, K.R., 2013. Effect of long term no-till and conventional tillage practices on soil quality. Soil Tillage Res. 131, 28–35.

Beraldo, J.M.G., Scannavino Junior, F.A., Cruvinel, P.E., 2014. Application of x-ray computed tomography in the evaluation of soil porosity in soil management systems. Eng. Agric. 34, 1162–1174.

Blanco-Canqui, H., Gantzer, C.J., Anderson, S.H., Alberts, E.E., 2004. Tillage and crop influences on physical properties for an Epiaqualf. Soil Sci. Soc. Am. J. 68, 567–576.

Blanco-Canqui, H., Lal, R., 2007. Regional assessment of soil compaction and structural properties under no-tillage farming. Soil Sci. Soc. Am. J. 71, 1770–1778.

Blanco-Canqui, H., Wienhold, B.J., Jin, V.L., Schmer, M.R., Kibet, L.C., 2017. Long-term tillage impact on soil hydraulic properties. Soil Tillage Res. 170, 38–42.

Borges, J.A.R., Pires, L.F., Cássaro, F.A.M., Auler, A.C., Rosa, J.A., Heck, R.J., Roque, W.L., 2018. X-ray computed tomography for assessing the effect of tillage systems on topsoil morphological attributes. Soil Tillage Res. (*submitted to publication*).

Bouma, J., Jongerius, A., Boersma, O.H., Jager, A., Schoonderbeek, D., 1977. The function of different types of macropores during saturated flow through four swelling soil horizons. Soil Sci. Soc. Am. J. 41, 945–950.

583 Buczko, U., Bens, O., Huttl, R.F., 2006. Tillage effects on hydraulic properties and
584 macroporosity in silty and sandy soils. Soil Sci. Soc. Am. J. 70, 1998–2007.

585 Bullock, P., Thomasson, A.J., 1979. Rothamsted studies of soil structure, II.
586 Measurement and characterisation of macroporosity by image analysis and
587 comparison with data from water retention measurements. J. Soil Sci. 30, 391–
588 413.

589 Bünemann, E.K., Bongiorno, G., Bai, Z., Creamer, R.E., De Deyn, G., de Goede, R.,
590 Fleskens, L., Geissen, V., Kuyper, T.W., Mäder, P., Pulleman, M., Sukkel, W., van
591 Groenigen, J.W., Brussaard, L., 2018. Soil quality – A critical review. Soil Biol.
592 Biochem. 120, 105–125.

593 Cameira, M.R., Fernando, R.M., Pereira, L.S., 2003. Soil macropore dynamics affected
594 by tillage and irrigation for a silty loam alluvial soil in southern Portugal. Soil Tillage
595 Res. 70, 131–140.

596 Carducci, C.E., Oliveira, G.C., Curi, N., Rossoni, D.F., Costa, A.L., Heck, R.J., 2014.
597 Spatial variability of pores in Oxidic Latosol under a conservation management
598 system with different gypsium doses. Ciênc. Agrotec. 38, 445–460.

599 Carducci, C.E., Zinn, Y.L., Rossoni, D.F., Heck, R.J., Oliveira, G.C., 2017. Visual
600 analysis and X-ray computed tomography for assessing the spatial variability of soil
601 structure in a cultivated Oxisol. Soil Tillage Res. 173, 15–23.

602 Cássaro, F.A.M., Borkowski, A.K., Pires, L.F., Rosa, J.A., Saab, S.C., 2011.
603 Characterization of a Brazilian clayey soil submitted to conventional and no-tillage
604 management practices using pore size distribution analysis. Soil Tillage Res. 111,
605 175–179.

606 Cavalieri, K.M.V., da Silva, A.P., Tormena, C.A., Leao, T.P., Dexter, A.R., Hakansson,
607 I., 2009. Long-term effects of no-tillage on dynamic soil physical properties in a
608 Rhodic Ferrasol in Paraná, Brazil. Soil Tillage Res. 103, 158–164.

609

610 Costa, L.F., Antonino, A.C.D., Heck, R.J., Coutinho, A.P., Vasconcelos, T.C.,
611 Machado, C.B., 2018. X-ray computed microtomography in the evaluation of the
612 porous system of soils. Rev. Bras. Eng. Agr. Amb. 22, 249–254.

613 Cunha, J.L.X.L., Coelho, M.E.H., Albuquerque, A.W., Silva, C.A., da Silva Junior, A.B.,
614 de Carvalho, I.D.E., 2015. Water infiltration rate in Yellow Latosol under different
615 soil management systems. Rev. Bras. Eng. Agr. Amb. 19, 1021–1027.

616 da Silva, V.R., Reichert, J.M., Reinert, D.J., Bortoluzzi, E.C., 2009. Soil water dynamics
617 related to the degree of compaction of two Brazilian oxisols under no-tillage. Rev.
618 Bras. Ci. Solo 33, 1097–1104.

619 da Silva, F.R., Albuquerque, J.A., da Costa, A., Fontoura, S.M.V., Bayer, C., Warmling,
620 M.I., 2016. Physical properties of a Hapludox after three decades under different
621 soil management systems. Rev. Bras. Ci. Solo 40, e0140331.

622 Dal Ferro, N., Charrier, P., Morari, F., 2014. Soil macro- and microstructure as affected
623 by different tillage systems and their effects on maize root growth. Soil Tillage Res.
624 140, 55–65.

625 Daraghmeh, O.A., Jensen, J.R., Petersen, C.T., 2008. Near-saturated hydraulic
626 properties in the surface layer of a sandy loam soil under conventional and
627 reduced tillage. Soil Sci. Soc. Am. J. 72, 1728–1737.

628 Daraghmeh, O.A., Jensen, J.R., Petersen, C.T., 2009. Soil structure stability under
629 conventional and reduced tillage in a sandy loam. Geoderma 150, 64–71.

630 Doube, M., Kłosowski, M.M., Arganda-Carreras, I., Cordelières, F.P., Dougherty, R.P.,
631 Jackson, J.S., Schmid, B., Hutchinson, J.R., Shefelbine, S.J., 2010. Bone 47,
632 1076–1079.

633 FEBRAPDP, 2013. Expansão da área cultivada em plantio direto. FEBRAPDP, Foz do
634 Iguaçu, Brasil. (available at: https://febrapdp.org.br/area-de-pd). Accessed on
635 November 2018.

636 Ferreira, T.R., Pires, L.F., Wildenschild, D., Heck, R.J., Antonino, A.C.D., 2018. X-ray
637 microtomography analysis of lime application effects on soil porous system.
638 Geoderma 324, 119–130.

639 Folegatti, M.V., Camponez do Brasil, R.P., Blanco, F.F., 2001. Sampling equipment for
640 soil bulk density determination tested in a Kandiudalfic Eutrudox and a Typic
641 Hapludox. Sci. Agri. 58, 833–838.

642 Franzluebbers, A.J., Stuedemann, J.A., Franklin, D.H., 2011. Water infiltration and
643 surface-soil structural properties as influenced by animal traffic in the Southern
644 Piedmond USA. Renew. Agric. Food Syst. 27, 256–265.

645 Fuentes, J.P., Flury, M., Bezdicek, D.F., 2004. Hydraulic properties in a silt loam soil
646 under natural prairie, conventional till, and no-till. Soil Sci. Soc. Am. J. 68, 1679–
647 1688.

648 Galdos, M.V., Pires, L.F., Cooper, H.V, Calonego, J.C, Rosolem, C.A. Mooney, S.J.
649 2018. Assessing the long-term effects of zero-tillage on the macroporosity of
650 Brazilian soils using X-ray Computed Tomography. Geoderma 337, 1126–1135.

651 Garbout, A., Munkholm, L.J., Hansen, S.B., 2013. Tillage effect on topsoil structural
652 quality assessed using X-ray CT soil cores and visual soil evaluation. Soil Tillage
653 Res. 128, 104–109.

654 Gee, G.W., Or, D., 2002. Particle-size analysis. In: Dane, J.H., Topp, G.C. (eds.)
655 Methods of Soil Analysis: Physical Methods. Soil Science Society of America Book
656 Series, Madison, USA. pp. 255–293.

657 Hammer, Ø., Harper, D.A.T., Ryan, P.D. 2001. PAST: Paleontological statistics
658 software package for education and data analysis. Palaeont. Elect. 4, 1–9.

Helliwell, J.R., Sturrock, C.J., Grayling, K.M., Tracy, S.R., Flavel, R.J., Young, I.M., Whalley, W.R., Mooney, S.J., 2013. Applications of X-ray computed tomography for examining biophysical interactions and structural development in soil systems: a review. Eur. J. Soil Sci. 64, 279–297.

Hernández Zubeldia, E., Ozelim, L.C.S.M., Brasil Cavalcante, A.L., Crestana, S., 2016. Cellular automata and X-ray microcomputed tomography images for generating artificial porous media. Int. J. Geomech. 16, 04015057.

Hillel, D., 2004. Introduction to environmental soil physics. Elsevier Academic Press, San Diego.

Imhoff, S., Ghiberto, P.J., Grioni, A., Gay, J.P., 2010. Porosity characterization of Argiudolls under different management systems in the Argentine Flat Pampa. Geoderma 158, 268–274.

Jabro, J.D., Sainju, U.M., Stevens, W.B., Lenssen, A.W., Evans, R.G., 2009. Long-term tillage influences on soil physical properties under dryland conditions in northeastern Montana. Arch. Agron. Soil Sci. 55, 633–640.

Jarvis, N., Forkman, J., Koestel, J., Kätterer, T., Larsbo, M., Taylor, A., 2017. Long-term effects of grass-clover leys on the structure of a silt loam soil in a cold climate. Agr. Ecosyst. Environ. 247, 319–328.

Jefferies, D.A., Heck, R.J., Thevathasan, N. V., Gordon, A.M., 2014. Characterizing soil surface structure in a temperate tree-based intercropping system using X-ray computed tomography. Agrofor. Syst. 88, 645–656.

Katsvairo, T., Cox, W.J., van Es, H., 2002. Tillage and rotation effects on soil physical characteristics. Agron. J. 94, 299–304.

Katuwal, S., Norgaard, T., Moldrup, P., Lamandé, M., Wildenschild, D., de Jonge, L.W., 2015. Linking air and water transport in intact soils to macropore characteristics inferred from X-ray computed tomography. Geoderma 237/238, 9–20.

685 Klein, V.A., Libardi, P.L., 2002. Densidade e distribuição do diametro dos poros de um
686 latossolo vermelho, sob diferentes sistems de uso e manejo (Bulk density and pore
687 size distribution of an Oxisol under different use and management systems). R.
688 Bras. Ci. Solo 26, 857–867.

689 Lima, H.V. de, Lima, C.L.R. de, Leão, T.P., Cooper, M., Silva, A.P. da, Romero, R.E.,
690 2005. Tráfego de máquinas agrícolas e alterações de bioporos em área sob pomar
691 de laranja (Agricultural machinery traffic and alterations in biopores under an
692 orange orchard). Rev. Bras. Ci. Solo 29, 677–684.

693 Mangalassery, S., Sjogersten, S., Sparkes, D.L., Sturrock, C.J., Craigon, J., Mooney,
694 S.J., 2014. To what extent can zero tillage lead to a reduction in greenhouse gas
695 emissions from temperate soils? Sci. Rep. 4, 4586.

696 Marchini, D.C., Ling, T.C., Alves, M.C., Crestana, S., Souto Filho, S.N., de Arruda,
697 O.G., 2015. Matéria orgânica, infiltração e imagens tomográficas de Latossolo em
698 recuperação sob diferentes tipos de manejo (Organic matter, water infiltration and
699 tomographic images of Latosol in reclamation under different managements). Rev.
700 Bras. Eng. Agr. Amb. 19, 574–580.

701 Martins, T., Saab, S.C., Milori, D., Brinatti, A.M., Rosa, J.A., Cassaro, F.A.M., Pires,
702 L.F., 2011. Soil organic matter humification under different tillage managements
703 evaluated by Laser Induced Fluorescence (LIF) and C/N ratio. Soil Tillage Res.
704 111, 231–235.

705 Mazurana, M., Levien, R., Inda Junior, A.V., Conte, O., Bressani, L.A., Muller, J., 2017.
706 Soil susceptibility to compaction under use conditions in southern Brazil. Ci.
707 Agrotec. 41, 60–71.

708 MINEROPAR, 2013. Serviço geológico do Paraná. Curitiba, Brasil. (available at:
709 http://www.mineropar.pr.gov.br/modules/conteudo/conteudo.php?conteudo=154).
710 Accessed on November 2018.

711 Munkholm, L.J., Hansen, E.M., 2012. Catch crop biomass production, nitrogen uptake
712 and root development under different tillage systems. Soil Use Managem. 28, 517–
713 529.

714 Munkholm, L.J., Heck, R.J., Deen, B., 2012. Soil pore characteristics assessed from X-
715 ray micro-CT derived images and correlations to soil friability. Geoderma 181/182,
716 22–29.

717 Muñoz-Ortega, F.J., San Jose Martinez, F., Caniego Monreal, F.J., 2015. Volume,
718 surface, connectivity and size distribution of soil pore space in CT images:
719 comparison of samples at different depths from nearby natural and tillage ares. Pre
720 Appl. Geophys. 172, 167–179.

721 Nelson, D.W., Sommers, L.E., 1982. Total carbon, organic carbon, and organic matter.
722 In: Page, A.L., Miller, R.H., Keeney, D.R. (eds.) Methods of Soil Analysis: Chemical
723 and Microbiological Properties. American Society of Agronomy, Soil Science
724 Society of America, Madison, USA. pp.539–580.

725 Odgaard, A., Gundersen, H.J.G., 1993. Quantification of connectivity in cancellous
726 bone, with special emphasis on 3-D reconstructions. Bone 14, 173–182.

727 Ogunwole, J.O., Pires, L.F., Shehu, B.M. 2015. Changes in the structure of a Nigerian
728 soil under different land management practices. Rev. Bras. Ci. Solo, 39, 830–840.

729 Otsu, N., 1979. A threshold selection method from gray-level histograms. IEEE
730 Transactions on Systems, Man and Cybernetics l. SMC-9, 62–6.

731 Pagenkemper, S.K., Puschmann, D.U., Peth, S., Horn, R., 2014. Investigation of time
732 dependent development of soil structure and formation of macropore networks as
733 affected by various precrop species. Int. Soil Wat. Cons. Res. 2, 51–66.

734 Pagenkemper, S.K., Athmann, M., Uteau, D., Kautz, T., Peth, S., Horn, R., 2015. The
735 effect of earthworm activity on soil bioporosity – Investigated with X-ray computed
736 tomography and endoscopy. Soil Tillage Res. 146, 79–88.

737 Pagliai, M., 1994. Micromorphology and soil management. In: Ringrose-Voase, A.J.,
738 Humphreys, G.S. (eds.) Soil Micromorphology: Studies in Management and
739 Genesis. Developments in Soil Science 22, Elsevier, Amsterdam. pp. 623–640.

740 Pagliai, M., Vignozi, N., Pellegrini, S., 2004. Soil structure and the effect of
741 management practices. Soil Tillage Res. 79, 131–143.

742 Passoni, S., Pires, L.F., Heck, R., Rosa, J.A., 2015. Three dimensional characterization
743 of soil macroporosity by x-ray microtomography. Rev. Bras. Ciência do Solo 39,
744 448–457.

745 Peña-Sancho, C., Lopez, M.V., Gracia, R., Moret-Fernandez, D., 2017. Effects of
746 tillage on the soil water retention curve during a fallow period of a semiarid dryland.
747 Soil Res. 55, 114–123.

748 Peth, S., Horn, R., Beckmann, F., Donath, T., Fischer, J., Smucker, A.J.M., 2008.
749 Three-dimensional quantification of intra-aggregate pore-space features using
750 synchrotron-radiation-based microtomography. Soil Sci. Soc. Am. J. 72, 897–907.

751 Pierret, A., Capowiez, Y., Belzunces, L., Moran, C.J., 2002. 3D reconstruction and
752 quantification of macropores using X-ray computed tomography and image
753 analysis. Geoderma 106, 247–271.

754 Pires, L.F., Borges, J.A.R., Rosa, J.A., Cooper, M., Heck, R., Passoni, S., Roque, W.L.,
755 2017. Soil structure changes induced by tillage systems. Soil Tillage Res. 165, 66–
756 79.

757 Rasband, W., 2007. ImageJ.1997–2007. U.S. National Institutes of Health, Bethesda,
758 MD, USA.

759 Reichert, J.M., Suzuki, L.E.A.S., Reinert, D.J., 2007. Compactação do solo em
760 sistemas agropecuários e florestais: Identificação, efeitos, limites críticos e
761 mitigação. Tópicos em Ciencia do Solo. pp. 49–134.

762 Rezanezhad, F., Quinton, W.L., Price, J.S., Elliot, T.R., Elrick, D., Shook, K.R., 2010.
763 Influence of pore size and geometry on peat unsaturated hydraulic conductivity
764 computed from 3D computed tomography image analysis. Hydrol. Process. 24,
765 2983–2994.

766 Rogasik, H., Schrader, S., Onasch, I., Kiesel, J., Gerke, H.H., 2014. Micro-scale dry
767 bulk density variation around earthworm (*Lumbricus terrestris* L.) burrows based on
768 X-ray computed tomography. Geoderma 213, 471–477.

769 Roque, W.L., Souza, A.C.A. de, Barbieri, D.X., 2009. The Euler-Poincaré characteristic
770 applied to identify low bone density from vertebral tomographic images. Rev. Bras.
771 Reumatol. 49, 140–152.

772 Roque, W.L., Arcaro, K., Lanfredi, R.B., 2012. Trabecular network tortuosity and
773 connectivity of distal radius from microtomographic images. Brazilian J. Biomed.
774 Eng. 28, 116–123.

775 Rosetti, K.V., Centurion, J.F., de Souza Neto, E.L., 2013. Physical quality of an Oxisol
776 afeter different periods of management systems. Rev. Bras. Ci. Solo 37, 1522–
777 1534.

778 Sá, J.C.M., Séguy, L., Tivet, F., Lal, R., Bouzinac, S., Borszowskei, P.R., Briedis, C.,
779 dos Santos, J.B., Hartman, D.C., Bertoloni, C.G., Rosa, J., Friedrich, T., 2015.
780 Carbon depletion by plowing and its restoration by no-till cropping systems in
781 Oxisols of Subtropical and Tropical agro-ecoregions in Brazil. Land Degrad.
782 Develop. 26, 531–543.

783 Soil Survey Staff, 2013. Simplified guide to soil taxonomy. USDA-Natural Resources
784 Conservation Service, National Soil Survey Center, Lincoln, USA.

785 Soracco, C.G., Lozano, L.A., Balbuena, R., Ressia, J.M., Filgueira, R.R., 2012.
786 Contribution of macroporosity to water flux of a soil under different tillage systems.
787 Rev. Bras. Ci. Solo 36, 1149–1155.

788 Soto-Gómez, D., Pérez-Rodríguez, P., Vázquez-Juiz, L., López-Periago, J.E.,
789 Paradelo, M., 2018. Linking pore network characteristics extracted from CT images
790 to the transport of solute and colloid tracers in soils under different tillage
791 managements. Soil Tillage Res. 177, 145–154.

792

793 Sterio, D.C., 1984. The unbiased estimation of number and sizes of arbitrary particles
794 using the disector. J. Microsc. 134, 127–136.

795 Strudley, M.W., Green, T.R, Ascough, J.C. 2008. Tillage effects on soil hydraulic
796 properties in space and time: State of the science. Soil Tillage Res. 99: 4–48.

797 Thurston, W.P., 1997. Three-dimensional Geometry and Topology, 1st ed. Princeton
798 University Press, Princeton.

799 Toriwaki, J., Yonekura, T., 2002. Euler number and connectivity indexes of a three
800 dimensional digital picture. Forma 17, 183–209.

801 Tseng, C.L, Alves, M.C., Crestana, S., 2018. Quantifying physical and structural soil
802 properties using X-ray microtomography. Geoderma 318, 78–87.

803 Vaz, C.M.P., de Maria, I.C., Lasso, P.O., Tuller, M., 2011. Evaluation of an advanced
804 benchtop micro-computed tomography system for quantifying porosities and pore-
805 size distributions of two Brazilian Oxisols. Soil Sci. Soc. Am. J. 75, 832–841.

806 Vogel, H.J., 1997. Morphological determination of pore connectivity as a function of
807 pore size using serial sections. Eur. J. Soil Sci. 48, 365–377.

808 Vogel, H.J., Kretzschmar, A., 1996. Topological characterization of pore space in soil –
809 sample preparation and digital image-processing. Geoderma 73, 23–38.

810 Wang, J., Guo, L., Bai, Z., Yang, L., 2016. Using computed tomography (CT) images
811 and multi-fractal theory to quantify the pore distribution of reconstructed soils
812 during ecological restoration in opencast coal-mine. Ecol. Engineer. 92, 148–157.

Yang, Y., Wu, J., Zhao, S., Han, Q., Pan, X., He, F., Chen, C., 2018. Assessment of the responses of soil pore properties to combined soil structure amendments using X-ray computed tomography. Sci. Rep. 8, 695.

Zhao, D., Xu, M., Liu, G., Yao, X., Tuo, D., Zhang, R., Xiao, T., Peng, G., 2017. Quantification of soil aggregate microstructure on abandoned cropland during vegetative succession using synchrotron radiation-based micro-computed tomography. Soil Tillage Res. 165, 239–246.

Zibilske, L.M., Bradford, J.M., 2007. Soil aggregation, aggregate carbon and nitrogen, and moisture retention induced by conservation tillage. Soil Sci. Soc. Am. J. 71, 793–802.

Zingg, T., 1935. Beitrag zur Schotteranalyse. Schweiz. Mineral. Petrogr. Mitt., 15, 39–140.

Figure Captions

Fig. 1. 3D reconstruction of selected soil cores (≈5.0 cm high and ≈4.8 cm inner diameter) and pore spaces for the different management systems studied. The soil sample images were reconstructed with a resolution of 35 μm.

Fig. 2. Morphological properties of the soil porous system of a Brazilian Rhodic Hapludox submitted to different management systems (F: secondary forest; ZT: zero-tillage; CT: conventional tillage; RT: reduced tillage). (a) Porosity (P). (b) Number of pores (NP). (c) Degree of anisotropy (DA). (d) Volumetric Euler-Poincare Characteristic (EPC_V). (e) Euler Number (EN) of the largest pore.

Fig. 3. Tortuosity of the soil porous system of a Brazilian Rhodic Hapludox submitted to different management systems (F: secondary forest; ZT: zero-tillage; CT: conventional tillage; RT: reduced tillage). (a) Average tortuosity (τ). (b) Tortuosity in the x direction (τ_x). (c) Tortuosity in the y direction (τ_y). (d) Tortuosity in the z direction (τ_z).

Fig. 4. Contribution of the different pore shapes to porosity for the Brazilian Rhodic Hapludox submitted to different management systems (F: secondary forest; ZT: zero-tillage; CT: conventional tillage; RT: reduced tillage). (a) Pores of equant (EQ) shape. (b) Pores of prolate (PR) shape. (c) Pores of oblate (OB) shape. (d) Pores of triaxial (TR) shape.

Fig. 5. Contribution of different sizes of pores to the volume of pores (VP) for the Brazilian Rhodic Hapludox submitted to different management systems (F: secondary

forest; ZT: zero-tillage; CT: conventional tillage; RT: reduced tillage). (a) Volume of pores between 0.0004 to 0.01 mm^3. (b) Volume of pores between 0.01 to 0.1 mm^3. (c) Volume of pores between 0.1 to 10 mm^3. (d) Volume of pores >10 mm^3.

Table 1. Texture (clay, silt, sand), macroporosity (Ma), microporosity (Mi) and organic carbon (OC) for the experimental areas under zero-tillage (ZT), conventional tillage (CT), reduced tillage (RT) and secondary forest (F) studied.

Property/ System	Clay	Silt	Sand	Ma	Mi	OC
		(g kg^{-1})		(cm^3 cm^{-3})		(g kg^{-1})
ZT	530	300	170	0.10	0.43	55.8
CT	610	220	170	0.19	0.37	31.7
RT	580	260	160	0.15	0.39	41.0
F	590	340	70	0.14	0.38	80.7

Ma: macroporosity; Mi: microporosity; OC: organic carbon. Mi was determined in undisturbed samples submitted at -6 kPa in an Eijkelkamp® suction table. The OC of the secondary forest was extracted from the work of Sá et al. (2015) for the surface layer (0-10 cm).

Table 2. Culture rotations per year for the experimental areas under zero-tillage (ZT), conventional tillage (CT) and reduced tillage (RT) studied.

Year	Management system and crop sequence	
	CT and RT	ZT
1981-1990	W/S	C/O/S - W/S/L - C/O/S - W/S/L - C/O/S - W/S
1990–1995	O/S - O/C - W/S - O/S - L/C	Similar to CT and RT
1995–2000	O/S - W/S - O+V/C - O/S - W/C	Similar to CT and RT
2000–2009	O/S – O/C - W/S - O+V/S - O/C - O/S - O/C - O/S - O/C - V/S	Similar to CT and RT
2009–2017	O/C	Similar to CT and RT

S: soybean (*Glycine max*); W: wheat (*Triticum aestivum* L.); O: oat or black oat (*Avena strigosa*); C: corn (*Zea mays* L.); V: vetch (*Vicia sativa*); L: Lupine (*Lupinus spp.*). The information presented in the table were adapted from Sá et al. (2015) and Martins et al. (2011)

Table 3. Indices utilized for the classification of pores in terms of shape.

Axes ratio	Shape			
	Equant (EQ)	Prolate (PR)	Oblate (OB)	Triaxial (TR)
Int./Maj.	≥2/3	<2/3	≥2/3	<2/3
Min./Int.	≥2/3	≥2/3	<2/3	<2/3

Int.: intermediate axis; Maj.: major axis; Min.: minor axis

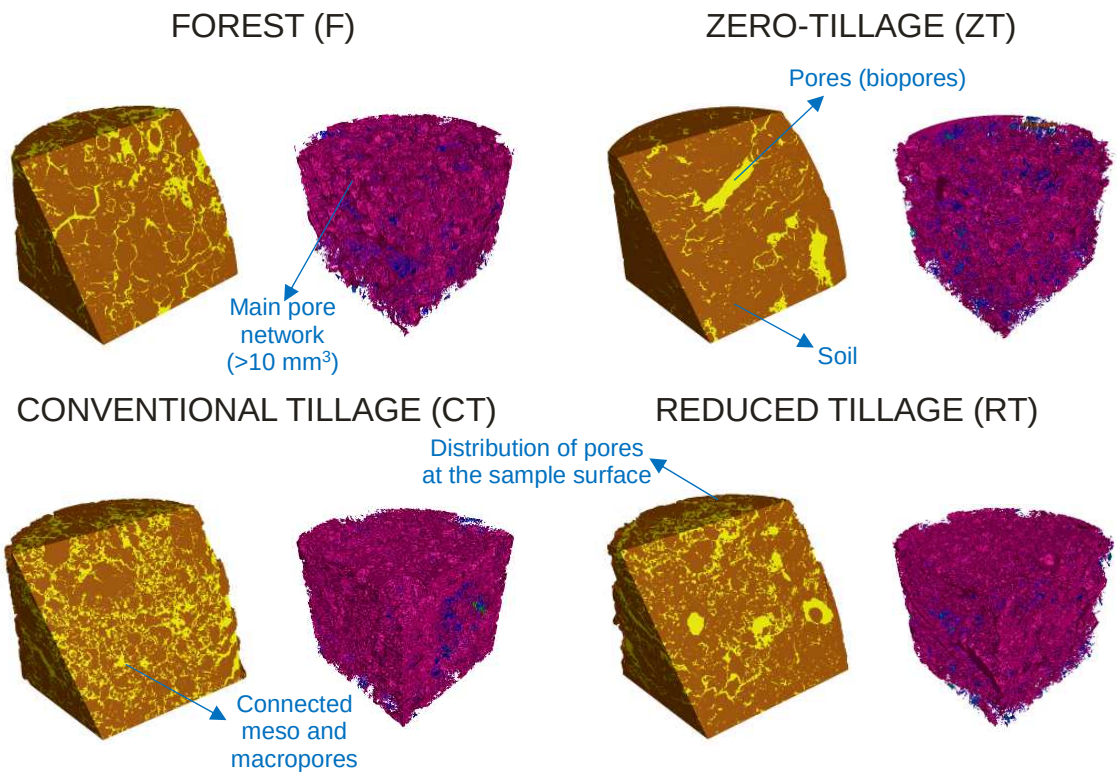

Fig. 1. 3D reconstruction of selected soil cores (5.0 cm high and 4.8 cm inner diameter) and pore spaces for the different management systems studied. The soil sample images were reconstructed with a resolution of 35 µm.

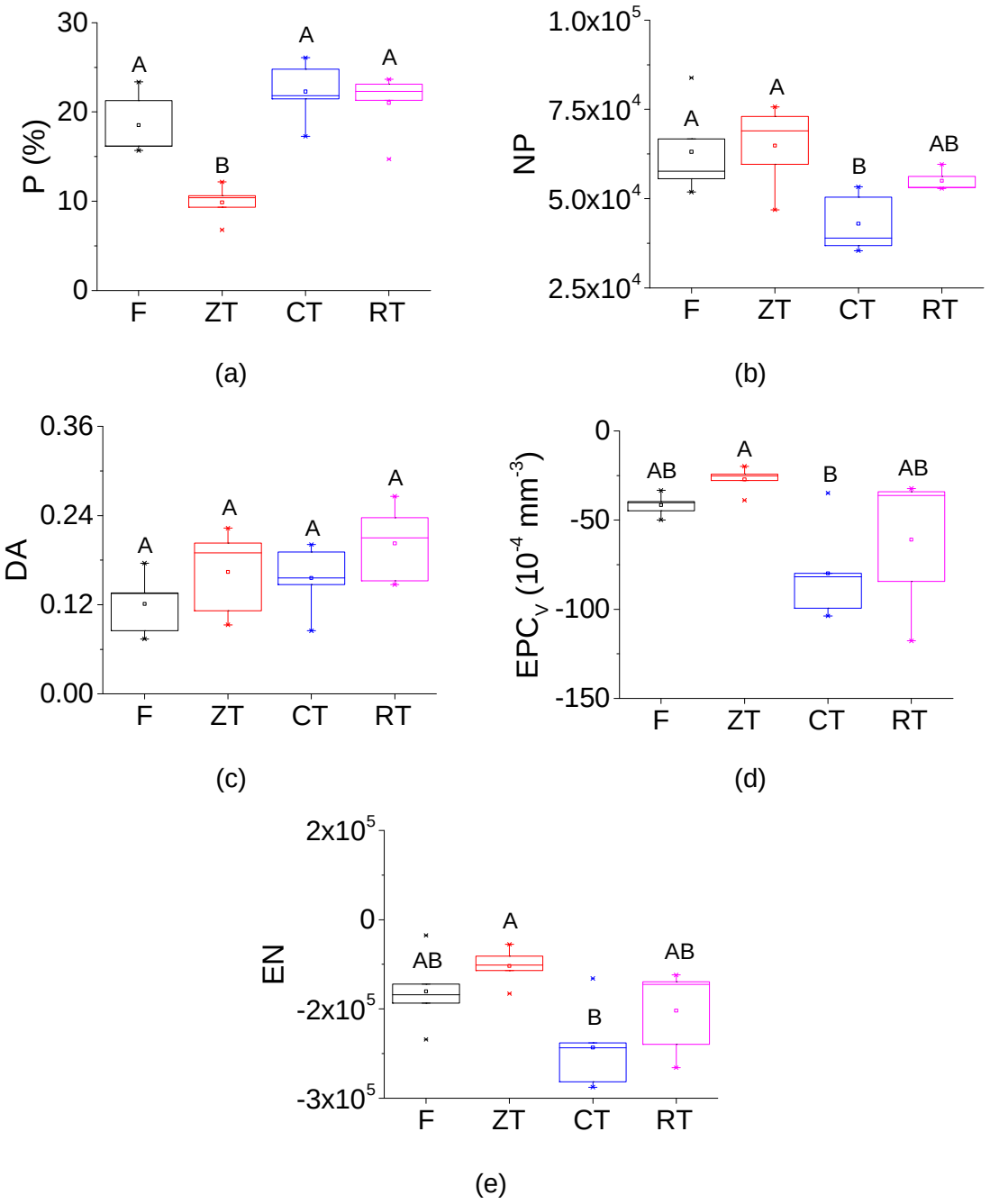

Fig. 2. Morphological properties of the soil porous system of a Brazilian Rhodic Hapludox submitted to different management systems (F: secondary forest; ZT: zero-tillage; CT: conventional tillage; RT: reduced tillage). (a) Porosity (P). (b) Number of pores (NP). (c) Degree of anisotropy (DA). (d) Volumetric Euler-Poincare characteristic (EPC_V). (e) Euler Number (EN) of the largest pore.

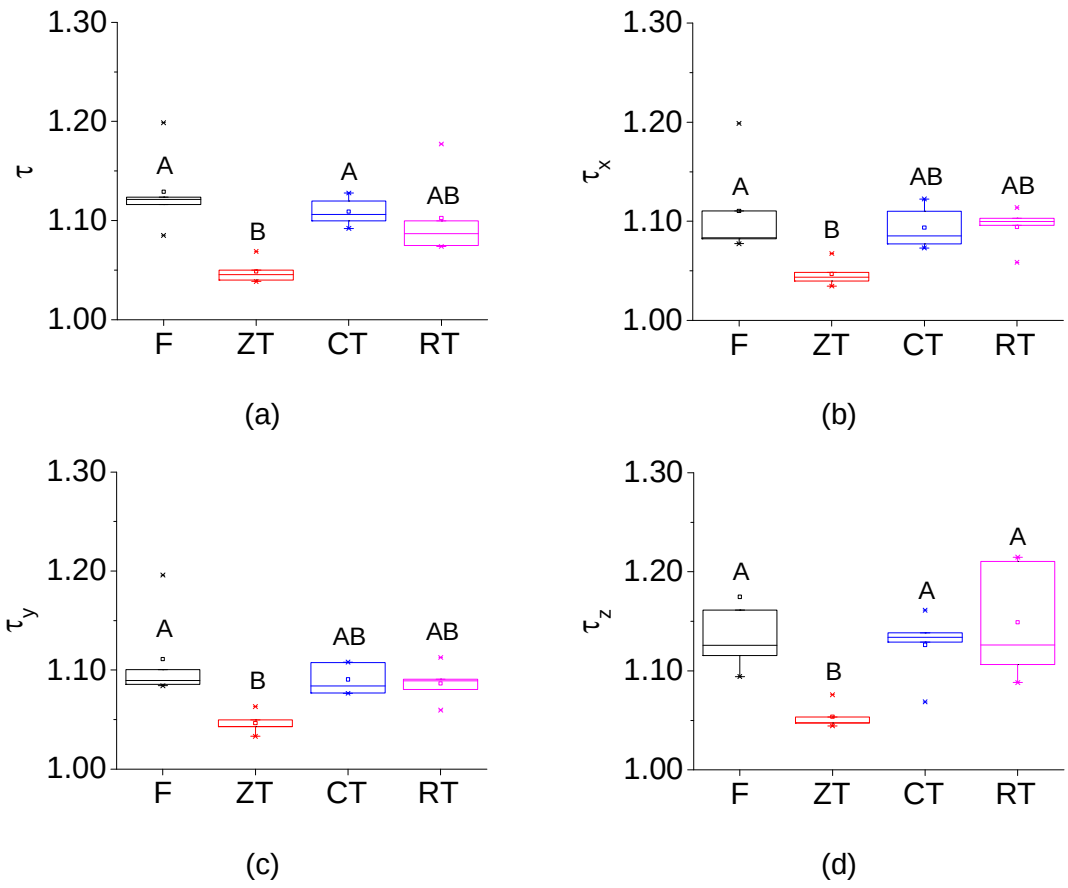

Fig. 3. Tortuosity of the soil porous system of a Brazilian Rhodic Hapludox submitted to different management systems (F: secondary forest; ZT: zero-tillage; CT: conventional tillage; RT: reduced tillage). (a) Average tortuosity (τ). (b) Tortuosity in the x direction (τ_x). (c) Tortuosity in the y direction (τ_y). (d) Tortuosity in the z direction (τ_z).

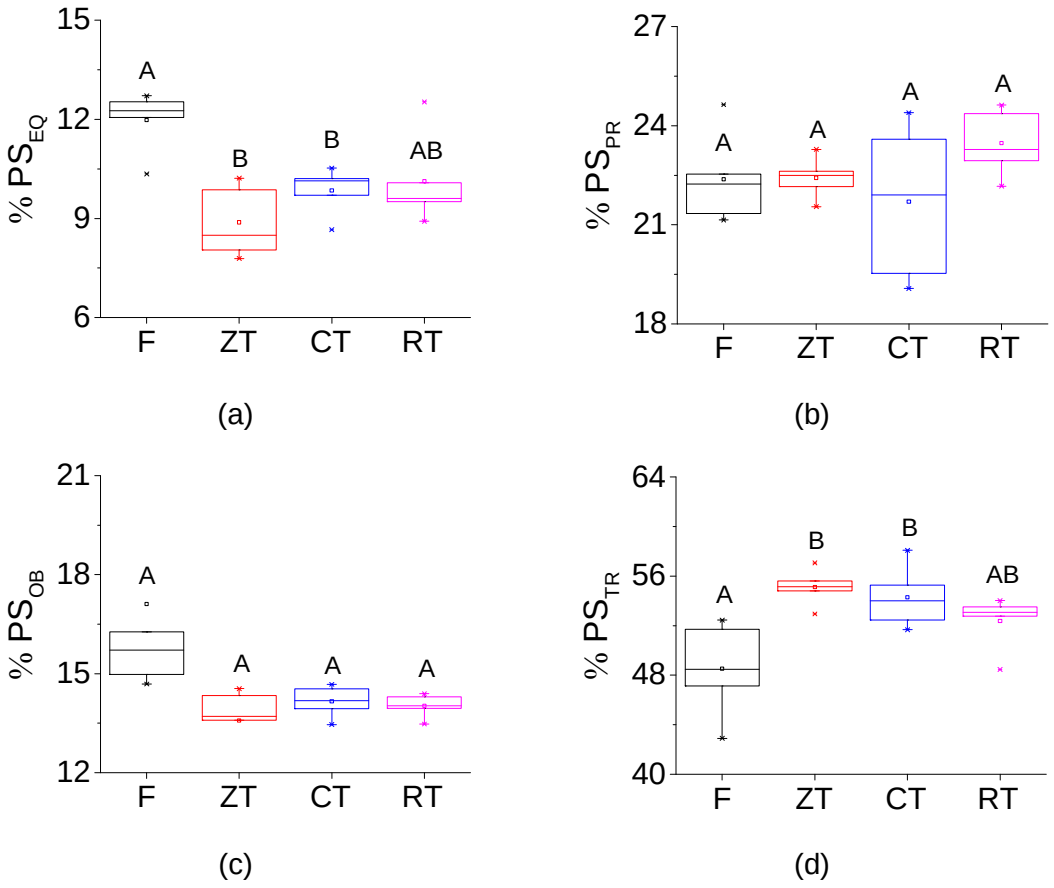

Fig. 4. Contribution of the different pore shapes to porosity for the Brazilian Rhodic Hapludox submitted to different management systems (F: secondary forest; ZT: zero-tillage; CT: conventional tillage; RT: reduced tillage). (a) Pores of equant (EQ) shape. (b) Pores of prolate (PR) shape. (c) Pores of oblate (OB) shape. (d) Pores of triaxial (TR) shape.

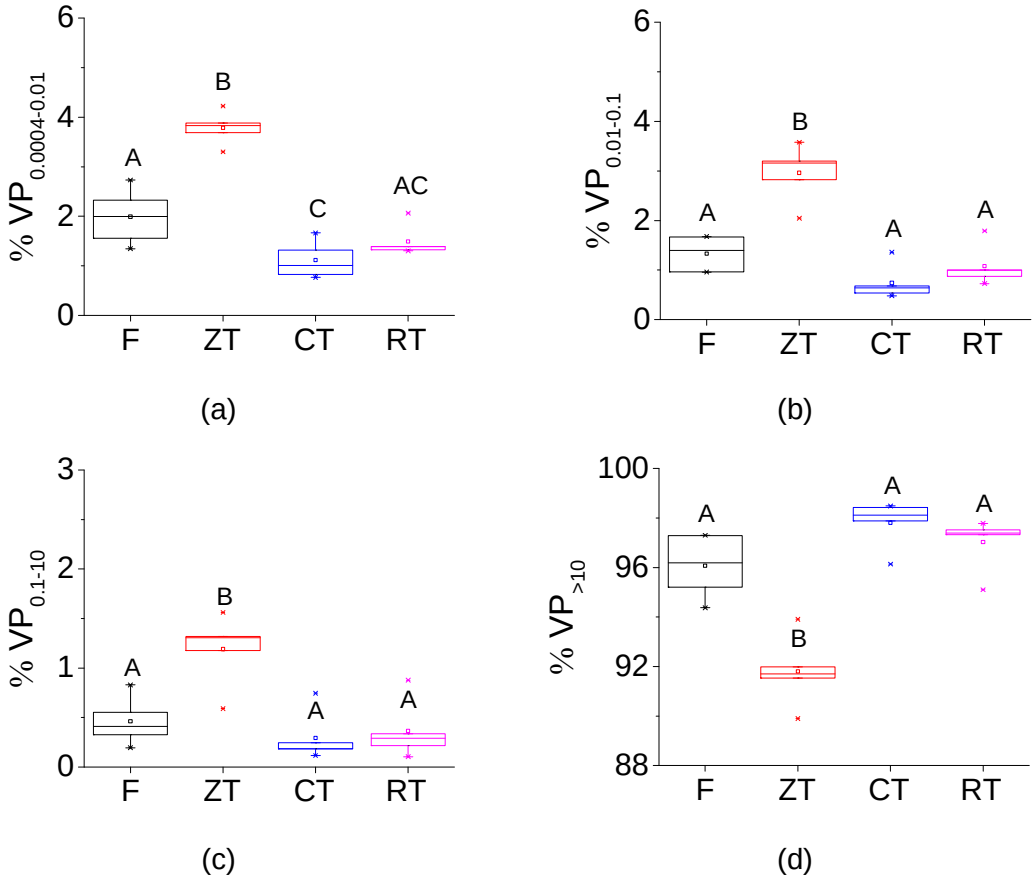

Fig. 5. Contribution of different sizes of pores to the volume of pores (VP) for the Brazilian Rhodic Hapludox submitted to different management systems (F: secondary forest; ZT: zero-tillage; CT: conventional tillage; RT: reduced tillage). (a) Volume of pores between 0.0004 to 0.01 mm^3. (b) Volume of pores between 0.01 to 0.1 mm^3. (c) Volume of pores between 0.1 to 10 mm^3. (d) Volume of pores >10 mm^3.